Pure appl. geophys. 163 (2006) 119–135
0033–4553/06/010119–17
DOI 10.1007/s00024-005-0011-0

Pure and Applied Geophysics

Seismic Hazard in Terms of Spectral Accelerations and Uniform Hazard Spectra in Northern Algeria

José A. Peláez,[1] M. Hamdache,[2] and Carlos López Casado[3]

Abstract—Seismic hazard in terms of spectral acceleration (*SA*) has been estimated for the first time in northern Algeria. For this purpose, we have used the spatially-smoothed seismicity approach. The present paper is intended to be a continuation of previous work in which we have evaluated the seismic hazard in terms of peak ground acceleration (*PGA*) using the same methodology. To perform these evaluations, four complete and Poissonian seismic models have been used. One of them considers earthquakes with magnitudes above M_S 6.5 in the last 300 years, that is, the most energetic seismicity in the region.
Firstly, seismic hazard maps in terms of *SA*, at periods of 0.1, 0.2, 0.3, 0.4, 0.5, 1.0, 1.5 and 2.0 sec, with 39.3% and 10% probability of exceedance in 50 years, have been obtained. Therefore, uniform hazard spectra (*UHS*) are computed and examined in detail for twelve of the most industrial and populated cities in northern Algeria. All the reported results in this study are for rock soil and 5% of damping.
It is noteworthy that, in the seismic hazard maps as well as in the *UHS* plots, we observe maximum *SA* values in the central area of the Tell. The higher values are reached in the Chleff region (previously El Asnam), specifically around the location of the destructive earthquakes of September 9, 1954 (M_S 6.8), and October 10, 1980 (M_S 7.3). These maximum values, 0.4 g and 1.0 g, are associated with periods of about 0.2 and 0.3 sec for return periods of 100 and 475 years, respectively.

Key words: Seismic hazard, spectral acceleration, uniform hazard spectra, spatially smoothed seismicity, Northern Algeria.

Introduction

In recent years, the interest of the scientific community regarding seismology and seismotectonics has greatly increased in Algeria, especially in the fields related to the seismic risk assessment of urban seismic areas and its possible reduction. This is due to the fact that Algeria has experienced in the past, and also recently, several damaging earthquakes (Fig. 1). Among them, those located in the vicinity of Algiers,

[1]Departamento de Física, Escuela Politécnica Superior, Universidad de Jaén, Campus de Las Lagunillas, Edificio A-3, 23071 Jaén, Spain. E-mail: japelaez@ujaen.es
[2]Départment Etudes et Surveillance Sismique, Centre de Recherche en Astronomie, Astrophysique et de Géophysique, B.P. 63, Bouzaréah, 16340 Algiers, Algeria.
[3]Departamento de Física Teórica y del Cosmos, Facultad de Ciencias, Universidad de Granada, Avda. Severo Ochoa, s/n. 18071 Granada, Spain.

which occurred on January 2, 1365 (I_{MM} = *IX*), February 3, 1716 (*XI*), December 3, 1735 (*VII*), March 17, 1756 (*VIII*), November 8, 1802 (*VIII*), June 18, 1847 (*VIII*) and November 5, 1924 (*VIII*), and those located in the vicinity of the city of Oran, on October 9, 1790 (*IX–X*) and May 21, 1889 (*VIII*). Moreover, for the last 50 years, the El Asnam region has suffered the most destructive and damaging earthquakes recorded in northern Algeria, namely those of September 9, 1954 (M_S 6.8) and October 10, 1980 (M_S 7.3).

The most significant and recent event was the May 21, 2003 (M_W 6.8) Algiers earthquake. Its epicenter was located offshore, at 50 km northeast of Algier. It caused extensive damage in the north-central part of Algeria, reaching a macroseismic intensity of IX–X in Zemmouri and Boumerdes, two small cities near the epicenter (HAMDACHE *et al.*, 2004).

In this context we focus on the importance of the seismic hazard assessment in terms of *SA* for this region, to improve reliable earthquake-resistant building codes. The design spectra are typically the starting points for both modern seismic design codes and assessment procedures. Also, this type of work is relevant for the design of buildings that cannot be modeled as systems with one degree of freedom, as well as for studies of their dynamic response.

The aim of this paper is to present the method and obtained results in the assessment of the seismic hazard in terms of *SA* maps and *UHS* plots in northern Algeria, using the spatially-smoothed seismicity approach. The present work is a continuation of the seismic hazard assessment in terms of *PGA* (Fig. 2) conducted by PELÁEZ *et al.* (2003, 2004) using the same approach. This methodology combines

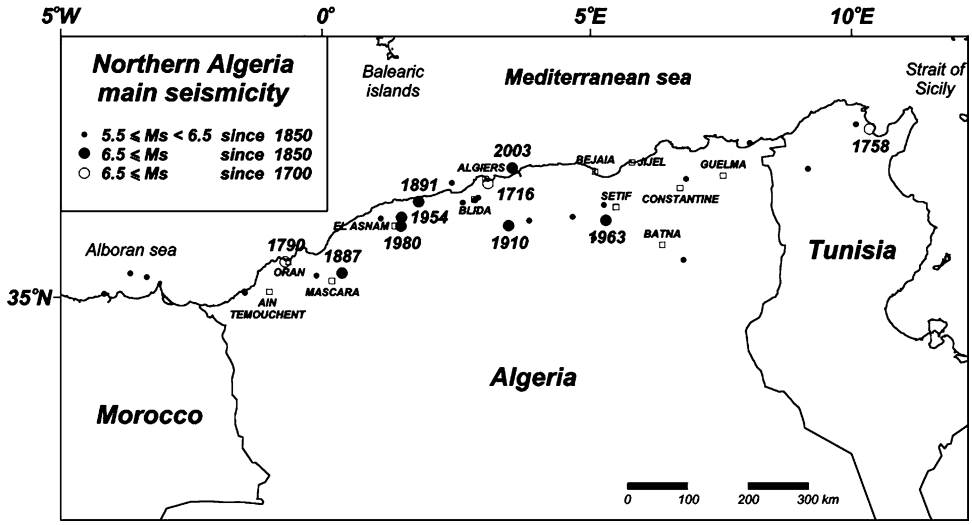

Figure 1
Seismicity map showing $5.5 \leq M_S < 6.5$ (small filled circles) and $M_S \geq 6.5$ (large filled circles) earthquakes since 1850 and $M_S \geq 6.5$ since 1700 (large open circles).

both parametric and nonparametric (non-zoning) probabilistic methods. It was introduced by FRANKEL (1995) and FRANKEL *et al.* (2000) to model the seismicity that cannot be assigned to specific geologic structures, usually termed as background or distributed seismicity. The original approach, with certain modifications, has been widely used (LAPAJNE *et al.*, 1997; PELÁEZ and LÓPEZ Casado, 2002; STIRLING *et al.*, 2002).

Tectonic Setting

Northern Algeria is located in the eastern part of the Ibero-Maghrebian region, in the westernmost Mediterranean area. This region is characterized by a complex seismotectonic pattern and moderate seismic activity associated with the convergence between the African and Eurasian plates. This seismicity is distributed over a wide area of deformation, as would be expected in a continent-continent collision. The tectonic of this region has been clearly summarized in PELÁEZ *et al.* (2003, 2004). In short, this region contains different geological domains whose formation is directly related to the multiple openings and closings of the Mediterranean Sea. Amongst the significant geological features related to interplate processes we can distinguish, from

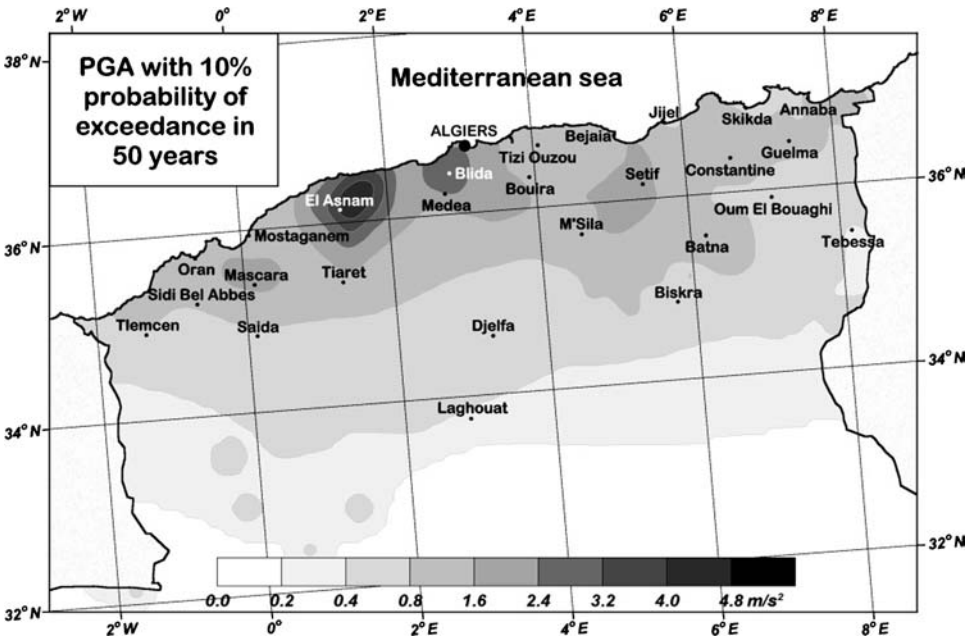

Figure 2
Seismic hazard in terms of PGA with 10% probability of exceedance in 50 years (modified from PELÁEZ *et al.*, 2003, 2004).

north to south, the Tell (Tell Atlas), the High Plateaus, the Sahara Atlas (Atlas Mountains system) and the Sahara platform (Fig. 3).

The Tell is part of an Alpine thrust system that extends from the Betic Cordilleras, in southern Spain, to Tunisia. After GUIRAUD *et al.* (1987), the late Eocene Tell is composed of numerous south-southeast directed thrust sheets and nappes consisting mainly of flysch, and with a minor amount of carbonate rocks. The rigid blocks, called mesetas in Morocco, were first formed during the Paleozoic Caldeonian-Hercynian orogeny. They consist of gently folded carbonate rocks with folding increasing in intensity in eastern Algeria, where the maximum Tellian thrusting occurred. The High Plateaus, which lie between the Tell and the Sahara Atlas, belong to the Atlas domain, and can be divided into two parts: 1) A southern section charaterized by relatively undeformed thick sequences of Mesozoic epicontinental deposits, and 2) a northern section with thinner Mesozoic sediments more deformed than the southern section, containing several allochthonous Tellian thrust sheets (ASFIANE and GALDEANO, 1995). The Atlas Mountains developed within the Proterozoic-Paleozoic Sahara Platform, and involved deformation of a continental margin that previously weakened during the formation of Triassic-Jurassic rift basins. Its position makes them an example of an intracontinental orogenic belt. These orogenic belts consist of Mesozoic rift sediments that were deformed into a series of large step folds. In the Saharian Atlas, the Mesozoic rift sediments were inverted into a major mountain range by thrust faults and block uplift tectonics. The

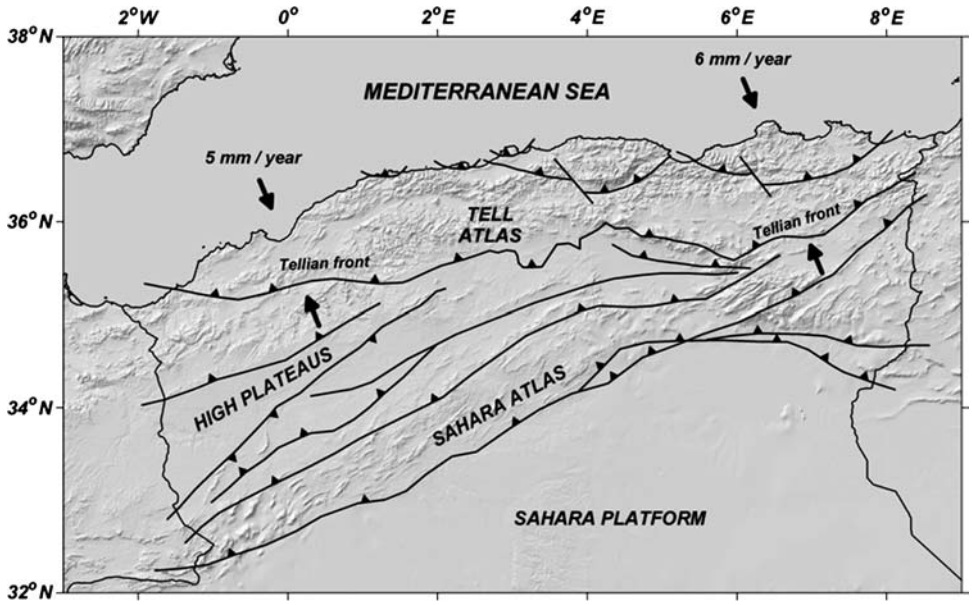

Figure 3
Tectonic sketch (simplified from BRACENE *et al.*, 2003).

southern boundary of the Atlas Mountains is termed the South Atlas front or flexure. This zone was thought to be a continent-wide transform fault and the boundary of the African continent. Recent studies (OUTTANI *et al.*, 1995) have shown that it consists of a series of discontinuous thrust and strike-slip faults, folds and simple flexures that are highly variable along its length.

The present geological configuration was a acquired during Mesozoic and Cenozoic extensional and compressional tectonic events, that were, as mentioned above, related to the opening and closing of the Mediterranean Sea (DEWEY *et al.*, 1989).

The Tell, where mostly seismicity occurred, is the eastern part of the Rif-Tell system, an active collision area between the Spain microplate and the African and Eurasian plates. It is composed, as in the case of the Betic Mountains, of internal and external zones, with different seismic characteristics. Since the early Cenozoic, this area is under a compressional regime, with a N-S to NW-SE convergence from the late Quaternary. Post-nappes basins present E-W to NE-SW fold reverse faults. Plate kinematic models for the region (ARGUS *et al.*, 1989; NEGREDO *et al.*, 2002; HENARES *et al.*, 2003, BUFORN *et al.*, 2004) show that this area absorbs 4 to 6 mm/year of crustal shortening (Fig. 3), with predominant dextral shearing, which accounts for the current seismicity. Main faults, with strike NE-SW, correspond to thrust fault dipping to NW often organized in echelon systems, such as the El Asnam and Tipaza faults (BEZZEGHOUD and BUFORN, 1999; AOUDIA *et al.*, 2000).

The seismicity in this region can be characterized by a continuous activity of moderate ($5 < M < 6.5$) to low ($M \leq 5$) earthquakes located in the vicinity of Quaternary basins (BEZZEGHOUD and BUFORN, 1999). Moreover, for the last 50 years the region was the site of destructive and large earthquakes, such as the 1954 and 1980 El Asnam (previously Orleansville) earthquakes (M_S 6.8 and M_S 7.3, respectively) and the 2003 Algiers earthquake (M_w 6.8).

Used Data

The earthquake catalog used in our work is the one developed by PELÁEZ *et al.* (2003). The catalog has been updated not only to include information until June 2003, as well as to a recent re-evaluation of several historical earthquakes by HARBI *et al.* (2003). It consists mainly of the updated data published by the Spanish Instituto Geográfico Nacional (IGN) (MEZCUA and MARTÍNEZ SOLARES, 1983), supplemented with the data published by the Algerian Centre de Recherche en Astronomie, Astrophysique et de Geophysique (CRAAG), the European-Mediterranean Seismological Centre (EMSC) and the US Geological Survey (USGS). The time span of the catalog, about 300 years, covers the known average recurrence time of the El Asnam fault for large earthquakes ($M > 7$) (MEGHRAOUI and DOUMAZ, 1996). Thus, although it could be improved, this catalog provides us with a good

reference frame for the seismic hazard computation. We have analyzed its completeness and Poissonian character, which is a key step to set up the four seismic models considered for the seismic hazard computation. These models will be explained below.

The main limitation of our assessment was not being able to include faults as seismic sources. In this region, only the above mentioned El Asnam fault has a known recurrence relationship, using paleoseismic data, for large earthquakes. It has been included in our assessment through the catalog, *i.e.*, the historic seismicity. The data available for other faults is very scarce, and do not include paleoseismic events nor instrumental earthquakes assigned to them.

The delimitation in seismic sources is the one proposed by PELÁEZ *et al.* (2003). Concerning northern Algeria, information pertaining to the delimitation by HAMDACHE (1998) and AOUDIA *et al.* (2000) also has been used. In northeastern Morocco and northern Tunisia, the source zones have been defined, taking more into account the seismic information rather than the geological context (seismicity sources). We did so just to incorporate the contribution of the seismicity of these regions. Each of the proposed seismic sources has been characterized by its respective b and $m_{\max}$ parameters of the truncated Gutenberg-Richter relationship. The resulting values can be consulted in PELÁEZ *et al.* (2003, 2004). Although it is not as important as in the parametric approach, the b and $m_{\max}$ values have been smoothed using the BENDER's (1986) procedure.

Our assessment needs, evidently, an appropriate attenuation relationship for spectral accelerations. Owing to the rate of great earthquakes in northern Algeria, as well as to the non-existence of an available strong motion regional database, we have insufficient reliable data on strong ground motion to perform a specific attenuation model. For these reasons, we have adopted here the spectral attenuation relationships for rock ($V_S > 750$ m/s), damped at 5%, developed by AMBRASSEYS *et al.* (1996) (Fig. 3). Although the data set used to establish these relationships is not uniform (LEE, 1997), the fact that these authors use several strong ground motion accelerograms recorded in northern Algeria makes them, probably, the most appropriate for this region.

Considering the completeness and Poissonian character of our catalog, as mentioned before, four seismic models have been established (PELÁEZ *et al.*, 2003, 2004): 1) earthquakes with magnitude above M_S 2.5 after 1960, 2) those with magnitude above M_S 3.5 after 1920, 3) those with magnitude above M_S 5.5 after 1850, and 4) those with magnitude above M_S 6.5 after 1700. We show in Figure 1 the seismicity included in the last two models, that is, the most energetic in this region during the last 300 years. The spatially smoothed seismicity approach adopted in our seismic hazard assessment requires to complete and normalize the seismicity included in the four previous models. These requirements are due to: 1) The fact that the minimum magnitude chosen for computation is M_S 2.5, *i.e.*, a value lower than the threshold magnitude of the models 2, 3 and 4, and 2) in order to preserve the seismic

activity rate in each of the models. In PELÁEZ *et al.* (2003) it has been shown that the model 2 has the highest annual rate above any magnitude, so that models 1, 3 and 4 have been normalized to it.

Methodology Outline

The region under study was first divided into square cells (10 km ×10 km), just as is common in this method, and we counted the number of earthquakes in each of them. The fraction of earthquakes in incremental intervals of magnitude was smoothed using a Gaussian function, thus incorporating the uncertainty in the earthquake location. This process has been carried out for each of the four seismic models considered. In FRANKEL (1995), FRANKEL *et al.* (2000), PELÁEZ and LÓPEZ CASADO (2002), PELÁEZ *et al.* (2002), and recently in LAPAJNE *et al.* (2003), for example, such assessment is described in detail.

From the smoothed earthquake number, we computed the seismic hazard using the well-known total probability theorem, expressed in terms of the rate of exceedance of a certain level of ground motion. To evaluate it, we consider, as quoted above, the attenuation relationship of AMBRASEYS *et al.* (1996) written in the form

$$\log y = C_1 + C_2 M + C_3 \log r \qquad r = \sqrt{d^2 + h_0^2}.$$

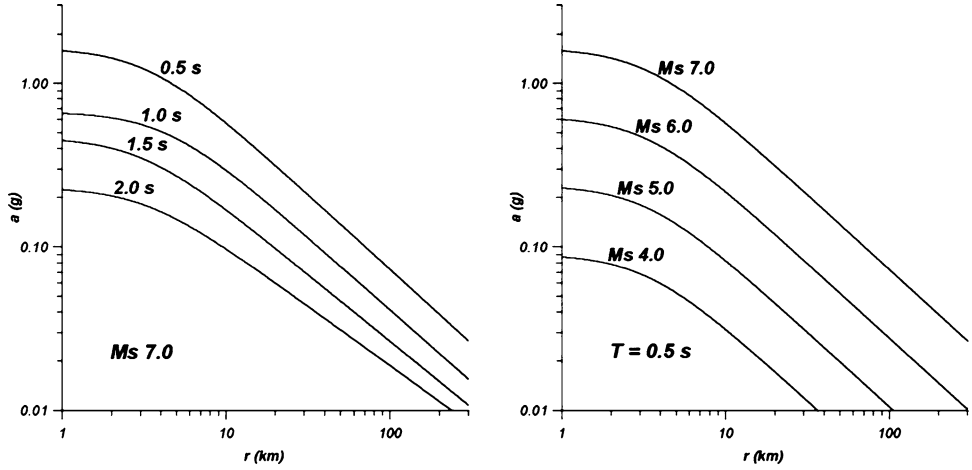

Figure 4
Predicted values using the AMBRASEYS *et al.* (1996) attenuation relationships for rock and damped at 5%. Left plot: Acceleration *vs.* distance for a M_S 7.0 earthquake and different periods. Right plot: Acceleration *vs.* distance for a 0.5 sec period and different magnitudes.

In this relationship C_1, C_2, C_3 and h_0 are coefficients depending on the period, log y is the dependent variable (log of spectral acceleration), M is the M_S magnitude, and d is the "Joyner-Boore distance".

The final result is obtained by weighting the seismic hazard result in each of the four seismic models separately. The procedure used to weight the different models remains mostly subjective and, in our case, it is based on the assumption that models having a time interval comparable to the return period, provide a higher contribution.

We derive SA values for rock ($V_S > 750$ m/s), corresponding to soil types A in the Eurocode 8 (EC 8, 1998) and S_1 in the Algerian building code (RPA-99, 2000), damped at 5%, at periods of 0.1, 0.2, 0.3, 0.4, 0.5, 1.0, 1.5 and 2.0 sec. If it becomes necessary, we recommend the procedure developed in the 2000 International Building Code (ICC, 2000) for adjusting 5%-damped spectra to other levels of damping. This adjustment is based on the relationship

$$SA_\eta = SA_{5\%}/C(\eta),$$

where $C(\eta)$ is the corresponding damping adjustment factor. We can use the C values proposed by NEWMARK and HALL (1982) or the more recent and reliable ones evaluated by NAEIM and KIRCHER (2001) (*v.g.*, $C(10\%) = 1.239$, $\sigma = 0.133$).

In addition to the seismic hazard assessment at different periods, we have calculated the *UHS* at twelve selected cities located in northern Algeria. In the *UHS* evaluation, we tried to obtain a high definition for the spectrum. To do so, and since the used attenuation relationships allow us, we have calculated the ordinate of the *UHS* at 0 sec (*PGA* value) and at 36 different period values ranging from 0.1–2.0 sec (between 0.1 and 0.5 sec with step size 0.02 sec, and between 0.5 and 2.0 sec with step size 0.1 sec).

Results

The obtained results at periods of 0.1, 0.2, 0.3, 0.4, 0.5, 1.0, 1.5 and 2.0 sec are plotted as contour maps, with 39.3% (Fig. 5) and 10% (Fig. 6) chance of exceedance in 50 years. These plots commonly show that maximum values occur in the central part of the Tell Atlas, around the El Asnam region, close to the location of the historical earthquake of January 15, 1891 (macroseismic magnitude M_S 7.0), and to the more important recent instrumental earthquakes of September 9, 1954 (M_S 6.8), and October 10, 1980 (M_S 7.3) (see Fig. 1). The maximum SA value in this region, for a return period of 475 years, is 0.95 g at 0.2 sec and 0.4 sec, and 1.07 g at 0.3 sec. This region appears clearly as the seismic source generating the higher seimic hazard level, independently of the return period being considered.

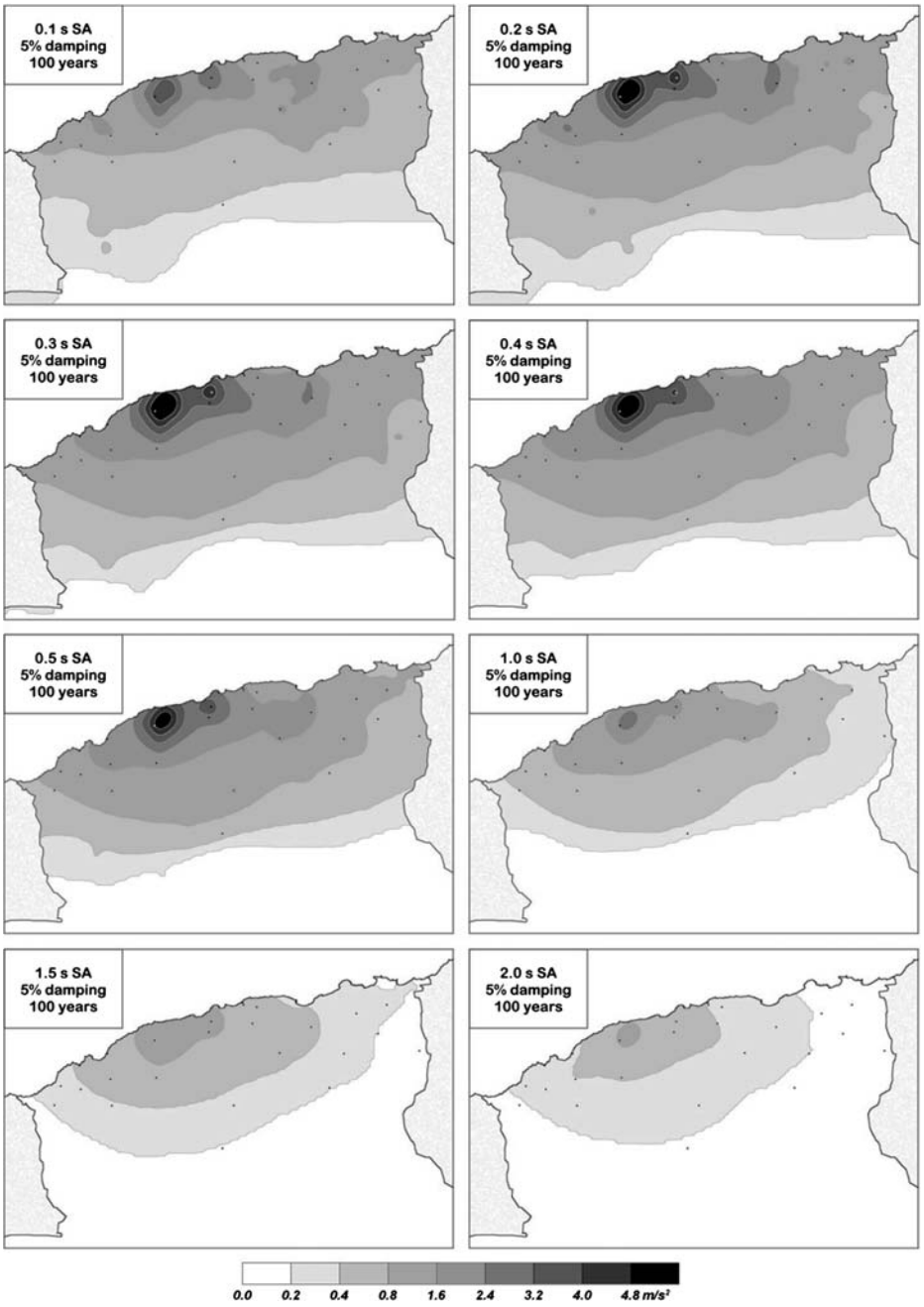

Figure 5
Seismic hazard in terms of *SA* (for rock and damped at 5%) with 39.3% probability of exceedance in 50 years (return period of 100 years). The maps show the results at periods of 0.1, 0.2, 0.3, 0.4, 0.5, 1.0, 1.5 and 2.0 sec. As a reference, the points are the cities in Figure 2.

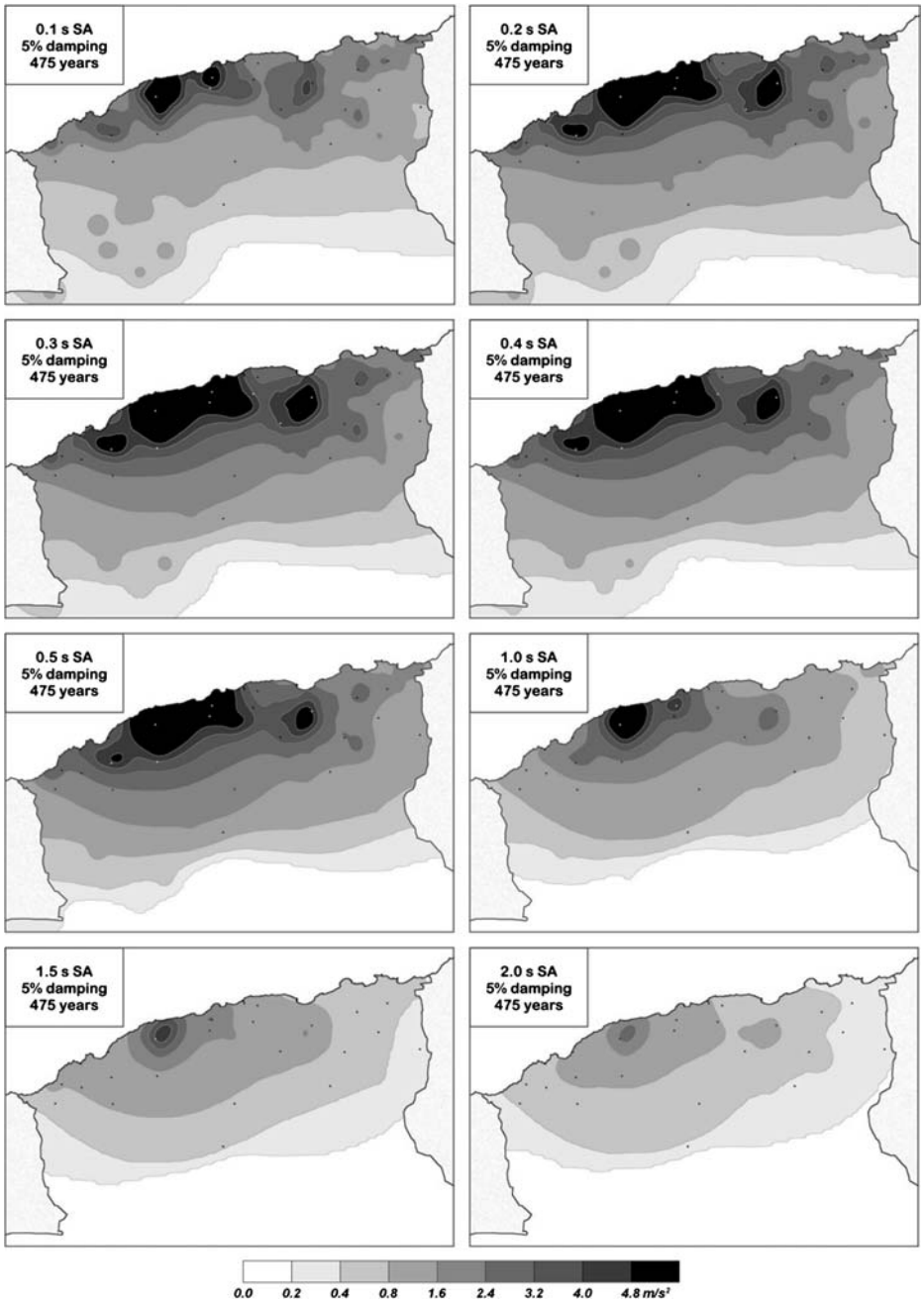

Figure 6
Seismic hazard in terms of *SA* (for rock and damped at 5%) with 10% probability of exceedance in 50 years (return period of 475 years). The maps show the results at periods of 0.1, 0.2, 0.3, 0.4, 0.5, 1.0, 1.5 and 2.0 sec. As a reference, the points are the cities in Figure 2.

A second seismic hazard nucleus, overlapping with the previous one, appears in the vicinity of Algiers, the capital of Algeria, specifically close to the border of the Mitidja Quaternary Basin. It coincides with the locations of some major earthquakes recorded in the vicinity of Algiers, such as the one of Algiers on February 3, 1716 (macroseismic magnitude M_S 7.0), the Tipaza earthquake of November 29, 1989 (M_S 5.7), and the most recent one of Algiers on May 21, 2003 (M_W 6.8) (see Fig. 1). The maximum SA value, for a return period of 475 years, is 0.67 g at 0.2 sec, 0.71 g at 0.3 sec, and 0.61 g at 0.4 sec.

Of less importance, another seismic hazard nucleus lies about 200 km to the east of the previous one. It is centered around the city of Setif, including the epicentral location of the earthquake of September 4, 1963 (m_b 6.3) (see Fig. 1). In this case, the maximum *SA* value, for a return period of 475 years, is 0.47 g at 0.2 sec, 0.48 g at 0.3 sec, and 0.41 g at 0.4 sec.

All these obtained values are in good agreement with the historical seismicity that northern Algeria experienced in the last 300 years (Fig. 1) and with our recent seismic hazard assessment in terms of *PGA* (Fig. 2).

It is interesting to emphasize that evident similarities appear between seismic hazard map morphologies for the two chosen return periods, 100 and 475 years, of course with different values. In addition to the shape of the isolines being similar for the different return periods, it seems that a common feature in the maps is the direction of the shape, elongated in agreement with the regional stress field (*e.g.*, HENARES *et al.*, 2003), especially in the Tell Atlas. Globally, in Figures 5 and 6 we observe clear bands with orientation ENE-WSW (practically parallel to the coast), with a decrease of the *SA* values toward the east and west of main hazard nuclei. These values decrease faster toward the south, in the direction of the Sahara Atlas, and they vanish at the Sahara Platform. We can see also in Figures 4 and 5, at periods above 1.0 to 1.5 sec, that seismic hazard is mostly due to the El Asnam seismic focus, particularly, for a return period of 100 years.

Figure 7 shows the *UHS* computed at the selected cities among the most important and populated in northern Algeria. As pointed out previously, the attenuation model developed by AMBRASEYS *et al.* (1996) allows us a high definition in the computation of the spectra (36 different ordinates are computed in the range 0.1 to 2.0 sec).

The analysis of Figure 7 reemphasizes the *SA* values at El Asnam as compared with the other ones. The maximum *SA* values at El Asnam for a return period of 475 years are 1.5 times those of the Blida, for example, which is the next one, of all cities selected, in terms of seismic hazard.

In Table 1 some *SA* characteristic values for the selected cities are shown. Besides *PGA* values (*SA* values at 0 sec), the maximum *SA* value and the period at which it is reached ($T_{\max}$) are presented. The results indicate that the greatest values of these two quantities are obtained in the city of El Asnam: 0.42 g for the *PGA*, and 1.00 g for the *SA* reached at 0.32 sec, for a return period of 475 years. At the city of Blida,

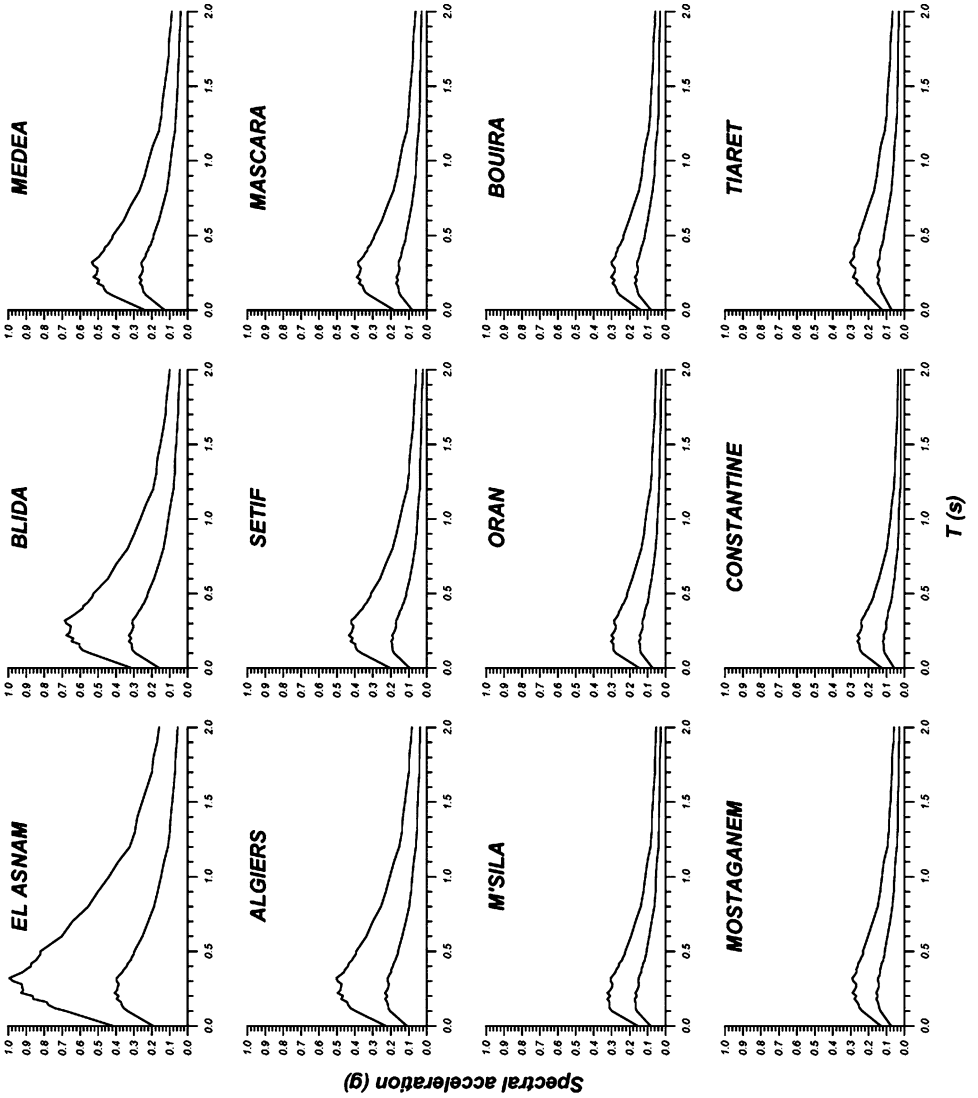

Figure 7
UHS (for rock and damped at 5%) with 39.3% and 10% probability of exceedance in 50 years for selected cities in northern Algeria.

the results for the same return period are, 0.32 g for the *PGA*, and 0.66 g for the *SA* at 0.32 sec. We observe that the maximum *SA* value in El Asnam, among others, takes place at a period of 0.32 sec, while on the contrary we have the cases of M'Sila, Oran and Constantine, where the maximum occurs at only 0.18 sec, in both cases for a return period of 475 years. It is clear that for the considered locations, the

Table 1

Mean PGA and maximum SA values for return periods of 100 and 475 years

City	100 years			475 years		
	PGA (g)	$SA_{T\max}$ (g)	$T_{\max}$ (s)	*PGA* (g)	$SA_{T\max}$ (g)	$T_{\max}$ (s)
El Asnam	0.194	0.408	0.22	0.418	0.995	0.32
Blida	0.160	0.329	0.22	0.315	0.658	0.32
Medea	0.129	0.271	0.22	0.240	0.535	0.32
Algiers	0.112	0.233	0.22	0.229	0.503	0.32
Setif	0.097	0.198	0.18	0.206	0.435	0.22
Mascara	0.081	0.170	0.18	0.184	0.390	0.22
M'Sila	0.084	0.173	0.18	0.157	0.325	0.18
Oran	0.073	0.148	0.18	0.148	0.304	0.18
Bouira	0.080	0.171	0.18	0.139	0.304	0.22
Mostaganem	0.076	0.158	0.22	0.132	0.291	0.32
Constantine	0.059	0.121	0.18	0.129	0.263	0.18
Tiaret	0.071	0.153	0.22	0.124	0.303	0.32

maximum *SA* values are observed at periods of about 0.2 to 0.3 sec, which appears as a characteristic period for the entire region.

We note that maximum *SA* values for a return period of 475 years are found for slighly higher periods than for 100 years (on average the difference is only 0.06 sec). This is due, in general, to the fact that when increasing the return period, more distant and energetic earthquakes contribute to the seismic hazard level at a given location. Moreover, the small increase in $T_{\max}$, on average, is connected to the fact of

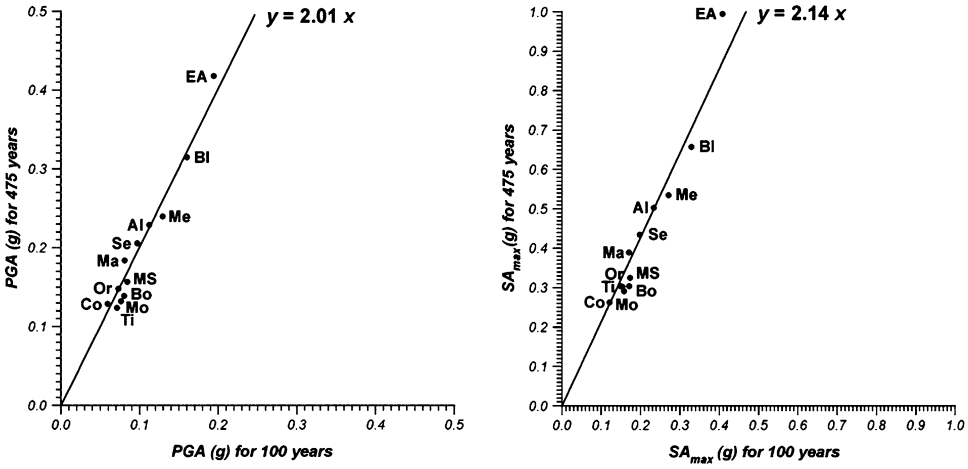

Figure 8

Acceleration with 39.3% *vs.* 10% probability of exceedance in 50 years for selected cities in northern Algeria. Left plot: for *PGA*. Right plot: for the maximum *UHS* value. EA: El Asnam. Bl: Blida. Me: Medea. Al: Algiers. Se: Setif. Ma: Mascara. MS: M'Sila. Or: Oran. Bo: Bouira. Mo: Mostaganem. Co: Constantine. Ti: Tiaret.

using a high attenuation relationship. As pointed out by AMBRASEYS *et al.* (1996), this attenuation model decays faster than, for example, the one developed for the western US by BOORE *et al.* (1993, 1994).

Figure 8 illustrates graphically the values in Table 1. The plots clearly reveal how, when the return period increases from 100 to 475 years, on average, the *PGA* doubles, while the maximum *SA* values are multiplied by 2.14.

In an attempt to describe and better characterize the obtained *UHS*, the half-width and mean slope values have been derived for each of the spectra (Table 2). We define these parameters as follows. The *UHS* half-width ($\Delta T_{1/2}$) is the period interval between the maximum *SA* and the following half maximum value (see Figure in Table 2). The *UHS* mean slope (*S*), is defined as the mean value of the *SA* slope across the previous interval. It is interesting to point out that this last parameter characterizes in all cases the *UHS* decrease in the range between 0.1 to 0.2 and 0.7 to 0.8 sec, illustrating how selective is this range.

In Table 2 we can see that *UHS* half-width values obtained for a return period of 475 years are greater than those obtained for 100 years (only 0.06 sec on average), that is, we obtain a slightly wider spectrum when increasing the return period. However, it seems that a clear correlation does not exist between the *UHS* half-width and the seismic hazard level (see Fig. 9). Nevertheless, the *UHS* mean slope value strongly correlates with the seismic hazard level, both for return periods of 100 and 475 years. In both cases the tendency is the same: higher seismic hazard level involves higher mean slope values (see Fig. 9). We can perform a linear fit, passing through the origin, which gives a slope value around 2. Finally, we mention that no correlation is observed between the half-width and the mean slope parameters (see Fig. 9).

Table 2

UHS half-width ($\Delta T_{1/2}$) *and mean slope* (*S*) *values for return periods of 100 and 475 years*

City	*100 years*		*475 years*	
	$\Delta T_{1/2}$ (s)	*S* (g/s)	$\Delta T_{1/2}$ (s)	*S* (g/s)
El Asnam	0.58	0.35	0.68	0.73
Blida	0.48	0.34	0.48	0.71
Medea	0.58	0.23	0.58	0.46
Algiers	0.58	0.20	0.58	0.43
Setif	0.42	0.24	0.58	0.38
Mascara	0.52	0.16	0.58	0.34
M'Sila	0.52	0.17	0.62	0.26
Oran	0.52	0.14	0.62	0.25
Bouira	0.62	0.14	0.58	0.26
Mostaganem	0.58	0.14	0.58	0.25
Constantine	0.42	0.14	0.52	0.25
Tiaret	0.58	0.13	0.68	0.22

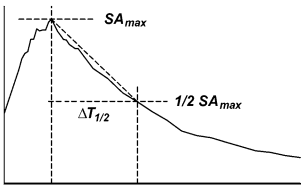

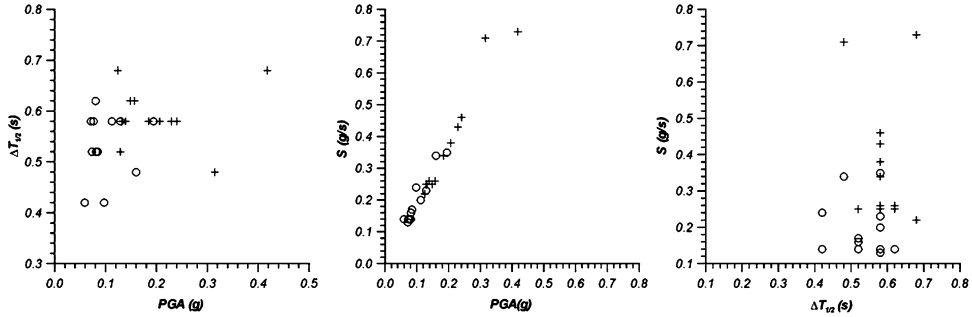

Figure 9
Plots of *UHS* half-width *vs. PGA* (left), *UHS* mean slope *vs. PGA* (center) and *UHS* half width *vs.* mean slope (right), using data from Tables 1 and 2, for return periods of 100 years (*o*) and 475 years (+).

Summary and Conclusions

In our study, the spatially-smoothed seismicity methodology has been used to derive probabilistic seismic hazard in northern Algeria for the first time in terms of the *SA* for rock soil and damped at 5%.

The catalog used has been compiled from different agencies (PELÁEZ *et al.*, 2003, 2004). Its completeness and Poissonian character make it the more reliable database to assess the probabilistic seismic hazard in this region to date. Previous probabilistic assessments published for the northern Algeria region, used catalogs which only spanned 90 years.

We have presented the obtained results as *SA* maps at different periods, with 39.3% and 10% in 50 years probability of exceedance. Thereafter, the *UHS* have been derived at twelve of the most important cities in northern Algeria.

Our results, in terms of *SA*, together with the previous *PGA* estimates by PELÁEZ *et al.* (2003, 2004), represent thus far the most complete seismic hazard assessment for this region, which is one of the most hazardous in the Ibero-Maghrebian area.

According to our work, the higher seismic hazard level occurs for the central part of the Tell, surrounding the El Asnam area, particularly in the vicinity of the location of large earthquakes recorded in the region. For a return period of 475 years, at El Asnam, we obtain 0.42 g for mean *PGA*, and 1.00 g at 0.32 sec for the *SA*. The seismic hazard assessment at the selected cities shows that maximum *SA* values are reached at periods ranging from 0.18 to 0.32 sec.

Seismic hazard maps computed in terms of *SA* clearly delineate bands of hazard intensity levels, decreasing predominantly from north to south. As quoted above, higher values are observed in the central part of the Tell, with some very well-defined areas and a slow decay toward the east (Tunisia) and the west (Morocco). Such areas appear to be related to the regional geological context, with known geological structures being potentially active. It is also important to remark that the

morphology of the seismic hazard level bands is clearly affected by the distribution of the seismicity, i.e., higher spatial density of moderate and large earthquakes implies a higher seismic hazard level.

Acknowledgments

This work was supported by the Spanish Seismic Hazard and Microzonification Research Group (RNM-0217) and the Algerian Centre de Recherche en Astronomie, Astrophysique et de Geophysique.

References

Ambraseys, N.N., Simpson, K.A., and Bommer, J.J. (1996), *Prediction of horizontal response spectra in Europe*, Earthquake Eng. Struct. Dyn. *25*, 371–400.

Aoudia, A., Vaccari, F., Suhadolc, P., and Meghraoui, M. (2000), *Seismogenic potential and earthquake hazard assessment in the Tell Atlas of Algeria*, J. Seismol. *4*, 79–98.

Argus, D.F., Gordon, R.G., De Mets, C., and Stein, S. (1989), *Closure of the Africa - Eurasia - North America plate motions circuit and tectonic of the Gloria fault*, J. Geophys. Res. *94*, 5585–5602.

Asfiane, F., and Galdeano, A. (1995), *The aeromagnetic map of northern Algeria: Processing and interpretation*, Earth Planet. Sci. Lett. *136*, 61–78.

Bender, B. (1986), *Modeling source zone boundary uncertainty in seismic hazard analysis*, Bull. Seismol. Soc. Am. *76*, 329–341.

Bezzeghoud, M. and Buforn, E. (1999), *Source parameters of 1992 Melilla (Spain, M_W=4.8), 1994 Alhoceima (Morocco, M_W=5.8), and 1994 Mascara (Algeria, M_W=5.7) earthquakes and seismotectonic implications*, Bull. Seismol. Soc. Am. *89*, 359–372.

Boore, D.M., Joyner, W.B., and Fumal, T.E. (1993), *Estimation of response spectra and peak accelerations from northern North American earthquakes; an interim report*, USGS Open-File Report 93-509, Denver, Colorado.

Boore, D.M., Joyner, W.B., and Fumal, T.E. (1994), *Estimation of response spectra and peak accelerations from northern North American earthquakes; an interim report; Part 2*, USGS Open-File Report 94-127, Denver, Colorado.

Bracene, R., Patriat, M., Ellouz, N., and Gaulier, J.M. (2003), *Subsidence history in basins of northern Algeria*, Sediment. Geol. *156*, 213–239.

Buforn, E., Bezzeghoud, M., Udías, A., and Pro, C. (2004), *Seismic sources on the Iberia-African plate boundary and their tectonic implications*, Pure Appl. Geophys. *161*, 623–646.

Dewey, J.F., Helman, M.L., Turco, E., Huston, D., and Knott, S.D.,. *Kinematics of the western Mediterranean*, In *Alpine Tectonics* (eds. Conward, M.P., Dietrich, D., and Park, R.G) (Special Publication of the Geological Society of London 45, 1989) pp. 265–283.

EC 8 (Eurocode 8) (1998), *Design provisions for earthquake resistance of structures – Part 1-1: General rules Seismic actions and general requirements for structures*, European Prestandard ENV 1998-1-1. Comité Européen de Normalisation, Brussels.

Frankel, A. (1995), *Mapping seismic hazard in the central and eastern United States*, Seism. Res. Lett. *66*, 8–21.

Frankel, A., Mueller, C.S., Barnhard, T.P., Leyendecker, E.V., Wesson, R.L., Harmsen, S.C., Klein, F.W., Perkins, D.M., Dickman, N.C., Hanson, S.L., and Hopper, M.G. (2000), *USGS national seismic hazard maps*, Earthquake Spectra *16*, 1–19.

Guiraud, R., Bellion, Y., Benkhelil, J., and Moreau, C. (1987), *Post-Hercynian tectonics in northern and western Africa*, Geol. J. *22*, 433–466.

HAMDACHE, M. (1998), *Seismic hazard assessment for the main seismogenic zones in north Algeria*, Pure Appl. Geophys. *152*, 281–314.

HAMDACHE, M., PELÁEZ, J.A. and YELLES-CHAUCHE, A.K. (2004), *The Algiers, Algeria earthquake (M_W 6.8) of 21 May 2003: Preliminary Report*, Seism. Res. Lett. *75* (3), 360–367.

HARBI, A., BENOUAR, D., and BENHALLOU, H. (2003), *Re-appraisal of seismicity and seismotectonics in the north-eastern Algeria. Part I: Review of historical seismicity*, J. Seismol. *7*, 115–136.

HENARES, J., LÓPEZ CASADO, C., SANZ DE GALDEANO, C., DELGADO, J. and PELÁEZ, J.A. (2003), *Stress fields in the Iberian-Maghrebi region*, J. Seismol. *7*, 65–78.

ICC (International Code Council) (2000), *2000 International Building Code*, ICC, Falls Church, Virginia.

LAPAJNE, J., MOTNIKAR, B.S., ZABUKOVEC, B., and ZUPANČIČ, P. (1997), *Spatially smoothed seismicity modelling of seismic hazard in Slovenia*, J. Seismol. *1*, 73–85.

LAPAJNE, J., MOTNIKAR, B.S., and ZUPAN∧cIÈ, P. (2003), *Probabilistic seismic hazard assessment methodology for distributed seismicity*, Bull. Seismol. Soc. Am. *93*, 2502–2515.

LEE, V.W. (1997), *Discussion: Prediction of horizontal response spectra in Europe*, Earthquake Eng. Struct. Dyn. *26*, 289–293.

MEGHRAOUI, M. and DOUMAZ, F. (1996), *Earthquake-induced flooding and paleoseismicity of the El Asnam, Algeria, fault-related fold*, J. Geophys. Res. *101*, 17617–17644.

MEZCUA, J. and MARTÍNEZ SOLARES, J.M. (1983), *Seismicity of the Ibero-Maghrebian area* (*in Spanish*), Instituto Geográfico Nacional Report, Madrid.

NAEIM, F. and KIRCHER, C.A. (2001), *On the damping adjustment factors for earthquake response spectra*, Struct. Design Tall Build. *10*, 361–369.

NEGREDO, A., BIRD, P., SANZ DE Galdeano, C., and BUFORN, E. (2002), *Neotectonic modeling of the Ibero-Maghrebian region*, J. Geophys. Res. *107*, B11, 2292, doi:10.1029/2001JB000743.

NEWMARK, N.M. and HALL, W.J. (1982), *Earthquake spectra and design*, Earthquake Engineering Research Institute, Oackland, California.

OUTTANI, F., ABDOUN, B., MERCIER, E., FRIZON DE LAMOTTE, D., and ANDRIEUX, J. (1995), *Kinematics of the south Atlas front, Algeria and Tunisia*, Tectonophysics *249*, 233–248.

PELÁEZ, J.A. and LÓPEZ CASADO, C. (2002), *Seismic hazard estimate at the Iberian Peninsula*, Pure Appl. Geophys. *159*, 2699–2713.

PELÁEZ, J.A., LÓPEZ CASADO, C., and HENARES, J. (2002), *Deaggregation in magnitude, distance and azimuth in the S and W of the Iberian Peninsula*, Bull. Seismol. Soc. Am. *92*, 2177–2185.

PELÁEZ, J.A., HAMDACHE, M., and LÓPEZ CASADO, C. (2003), *Seismic hazard in Northern Algeria using smoothed seismicity. Results for peak ground acceleration*, Tectonophysics *372*, 105–119.

PELÁEZ, J.A., HAMDACHE, M., and LÓPEZ CASADO, C. (2004), *Updating the probabilistic seismic hazard values of northern Algeria with the 21 May 2003 M 6.8 Algiers earthquake included*. Pure Appl. Geophys. *162*, 2163–2177.

RPA-99 (2000), *Règles Parasismiques Algériennes 1999*, Centre National de Recherche Apliquée en Génie Parasismique, Alger.

STIRLING, M.W., MCVERRY, G.H., and BERRYMAN, K.R. (2002), *A new seismic hazard model for New Zealand*, Bull. Seismol. Soc. Am. *92*, 1878–1903.

(Received October 25, 2004; accepted May 10, 2005)